What drives the growth of black holes?
Durham, 2010 July 26-29

The relation between circumnuclear star formation and black hole growth in the mid-IR and hard X-rays

Emanuele Nardini

Dipartimento di Fisica e Astronomia - Università di Firenze

INAF - Osservatorio Astrofisico di Arcetri

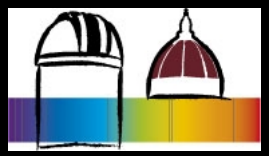

in collaboration with:

G. Risaliti, M. Salvati, E. Sani, ...

Outline

Search for evidence of the interplay
between nuclear activity and star formation
in the local Universe

1. Ultraluminous Infrared Galaxies
Quantitative study of the AGN/SB relation at extreme luminosities and dust obscuration

2. Narrow-Line Seyfert 1 Galaxies
Connection between SF and AGN at the higher end of the accretion rate distribution

1. Ultraluminous Infrared Galaxies

ULIRGs

$L_{IR} > 10^{12}\ L_{\odot}$
$L_{IR} \sim 60\text{-}95\%\ L_{bol}$

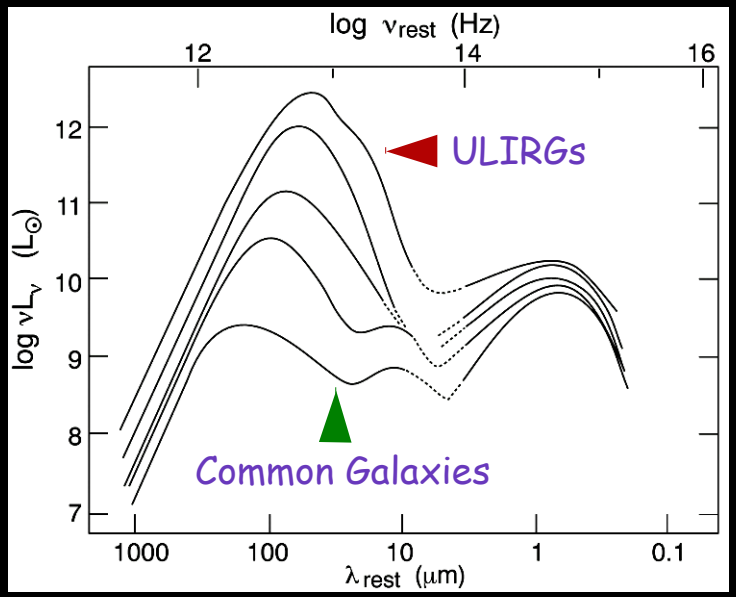

Sanders & Mirabel 96

Milky Way

$L_{IR} \sim 10^{10}\ L_{\odot}$
$L_{IR} \sim 10\text{-}30\%\ L_{bol}$

Huge IR emission related to interacting/merging systems

Energy source: starburst (SB) and/or accretion on to a supermassive black hole (AGN)

Local counterparts of the mid-IR/sub-mm galaxies dominating the energy output at high *z*

Disentangling SB and obscured AGN

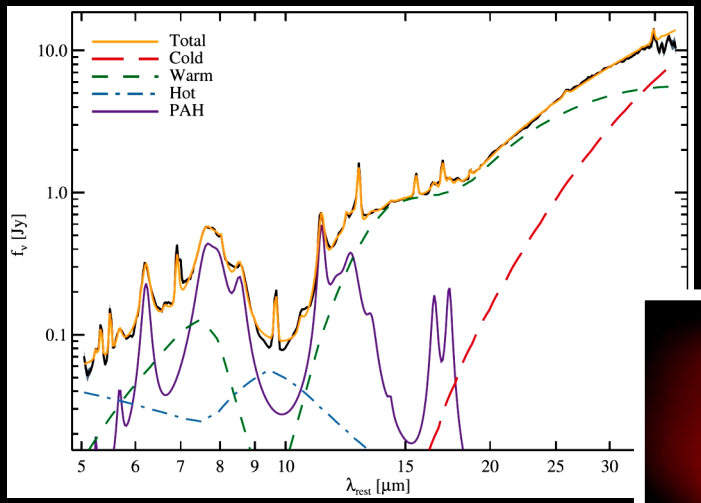

Armus+07

1) Optical emission lines (Veilleux+99, Yuan+10)

2) Mid-IR high-ionization lines (Genzel+98, Farrah+07)

3) Mid-IR SEDs (Laurent+00, Armus+07, Veilleux+09)

4) PAH features and Silicate absorption (Spoon+07)

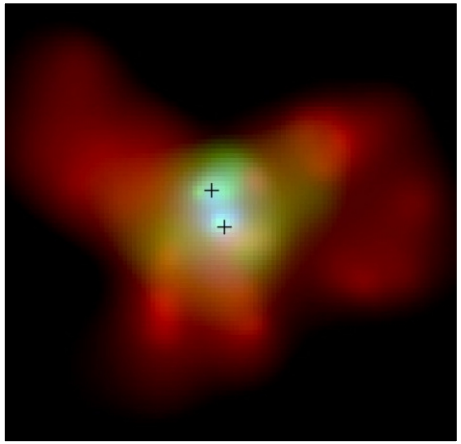

Komossa+03

5) X-ray spectral analysis (Franceschini+03, Teng+05)

6) X-ray imaging (Komossa+03)

Aim: to detect faint/obscured AGN components and to estimate their contribution to the IR luminosity

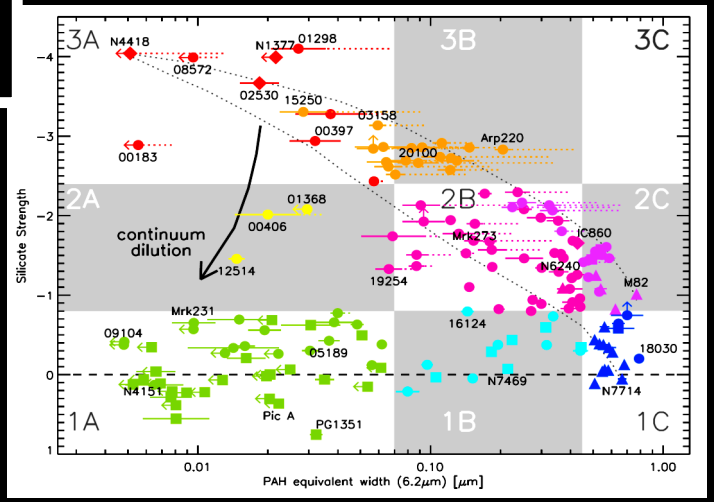

Spoon+07

AGN/SB spectral decomposition at 5-8 *μm*

- Diagnostic method: separation of the AGN/SB contribution to the observed emission of ULIRGs through spectral templates

- Why 5-8 *μm*: enhancement of the AGN over SB brightness ratio for equal bolometric luminosity due to the hot dust component, large difference between the average AGN/SB properties and little spectral dispersion observed within the separate classes

- Main results: SB events confirmed as the dominant power supply but AGN detection rate of ~70% - Sharp increase of the AGN contribution across the IR luminosity range - Strong evidence for elusive AGN missed by the standard optical diagnostics

- Elusive AGN population: follow-up X-ray observations of the most intriguing sources in this class (~10% of local ULIRGs)

References:

Spectral decomposition of SB and AGN in Spitzer-IRS spectra of local ULIRGs, Nardini+08 MNRAS
Exploring the AGN/SB content of local ULIRGs through 5-8 μm spectroscopy, Nardini+09 MNRAS
The role of nuclear activity as the power source of ULIRGs, Nardini+10 MNRAS

AGN/SB luminosity ratio in action

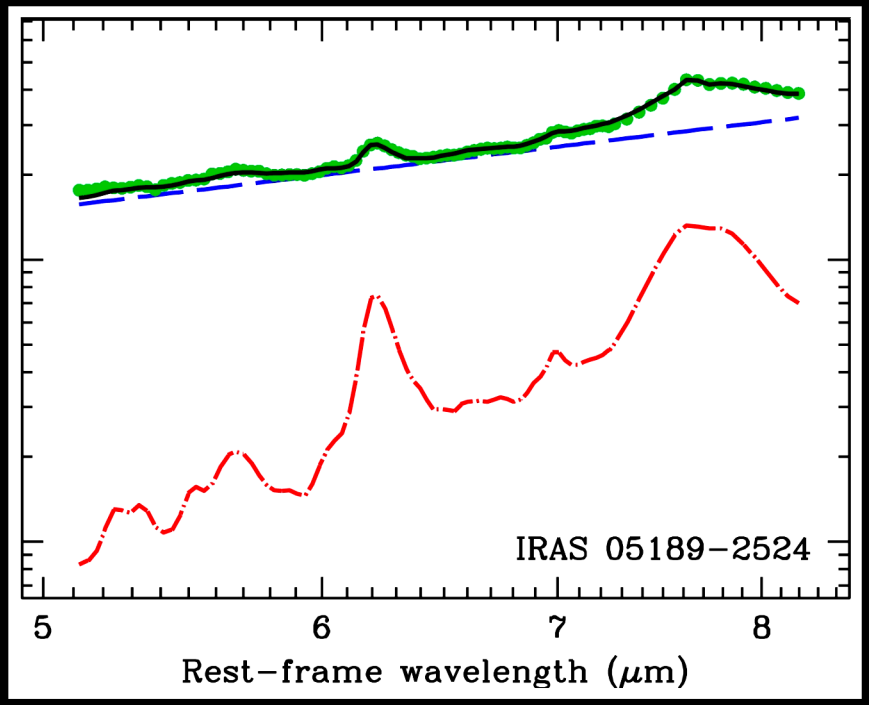

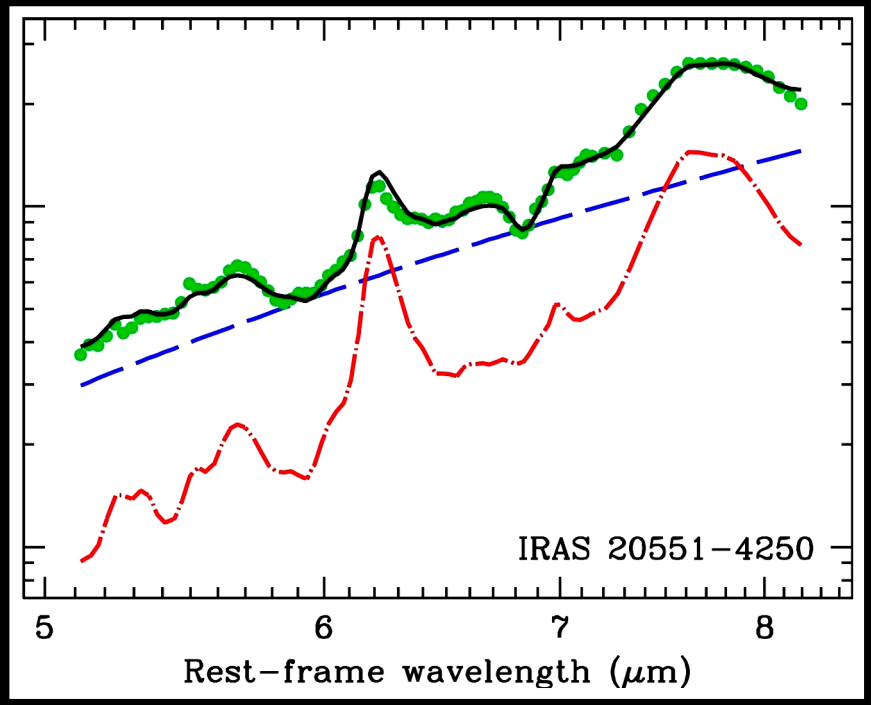

~70% Starburst
~30% unobscured AGN

~70% Starburst
~30% obscured AGN

Application: 1) Sample of 164 bright ULIRGs at $z \sim 0.02$-0.35
2) Acceptable fit for all the sources: spectral variations are due to the AGN and its obscuration 3) Estimate of the relative AGN/SB contribution to the *bolometric* luminosity

Results of the IR spectral decomposition

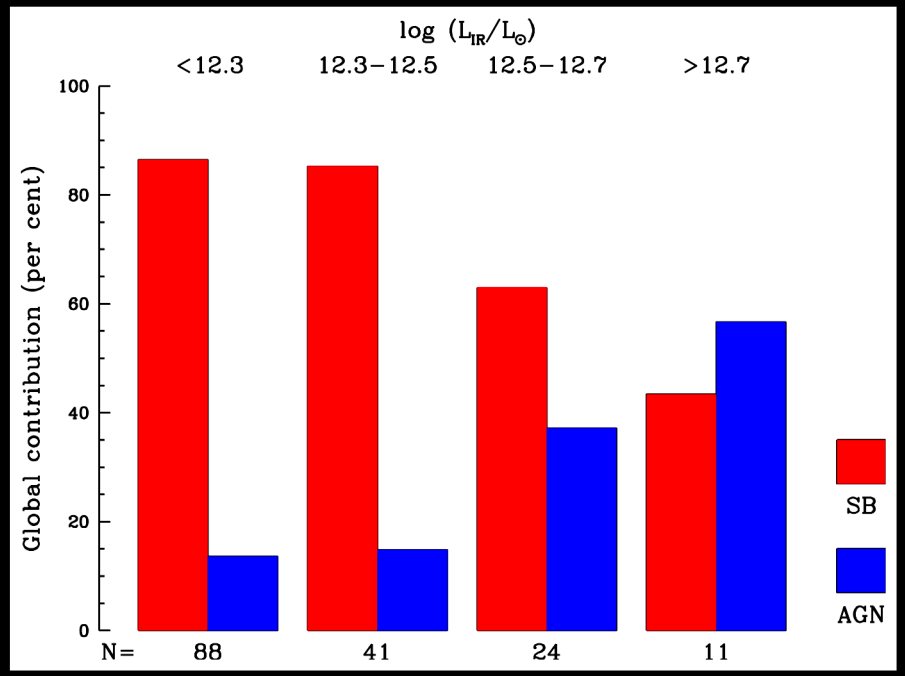

AGN contribution *v.*
IR luminosity:
Growing AGN significance with tentative evidence for non-uniformity: a hint of mutual AGN/SB feedback?

AGN contribution *v.*
Optical classification:
Powerful but highly obscured AGN are actually at work in many sources with no optical signature of nuclear activity

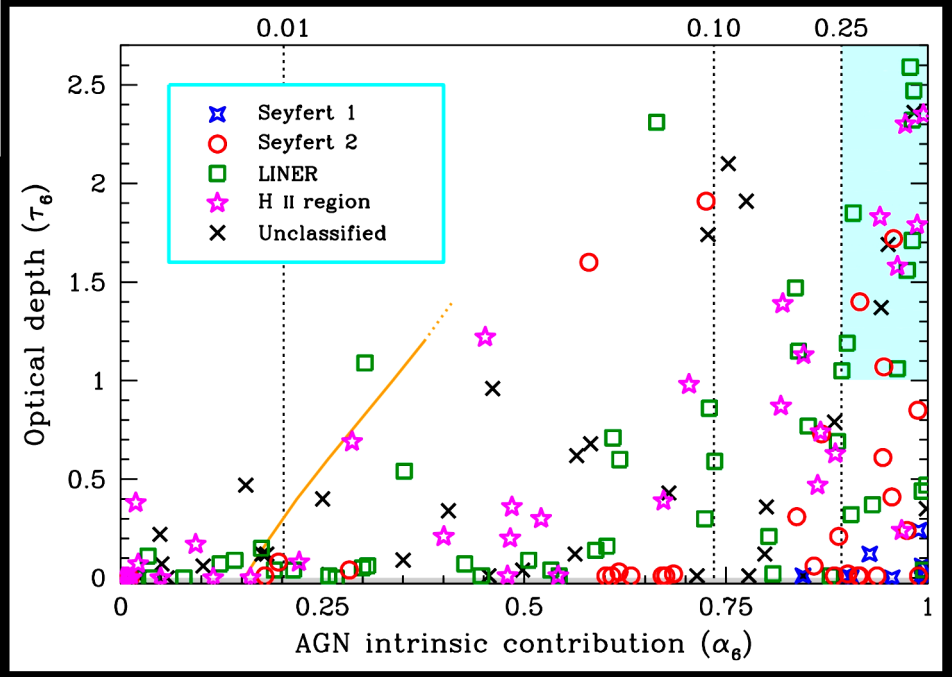

Expected X-ray emission of ULIRGs

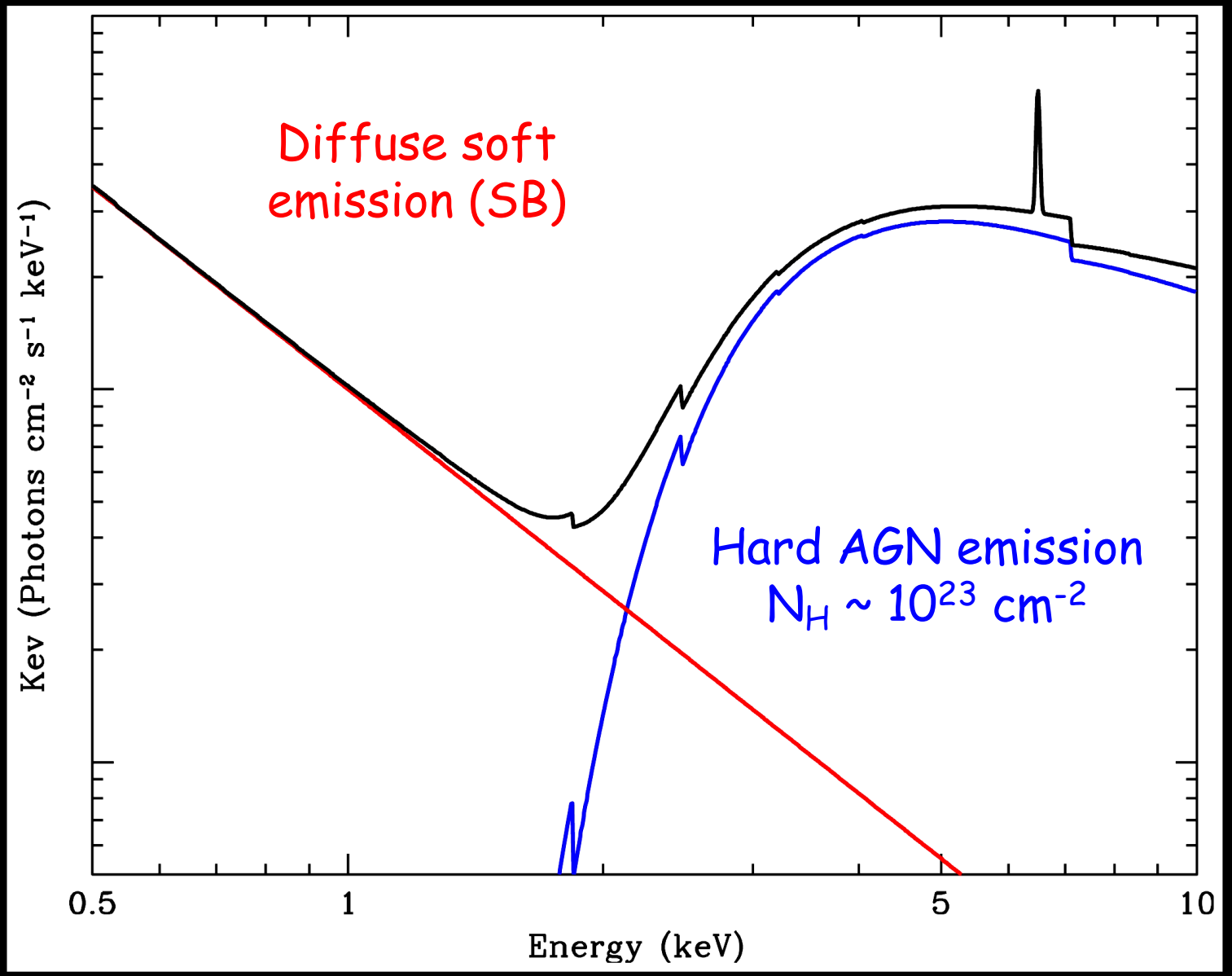

Expected X-ray emission of ULIRGs

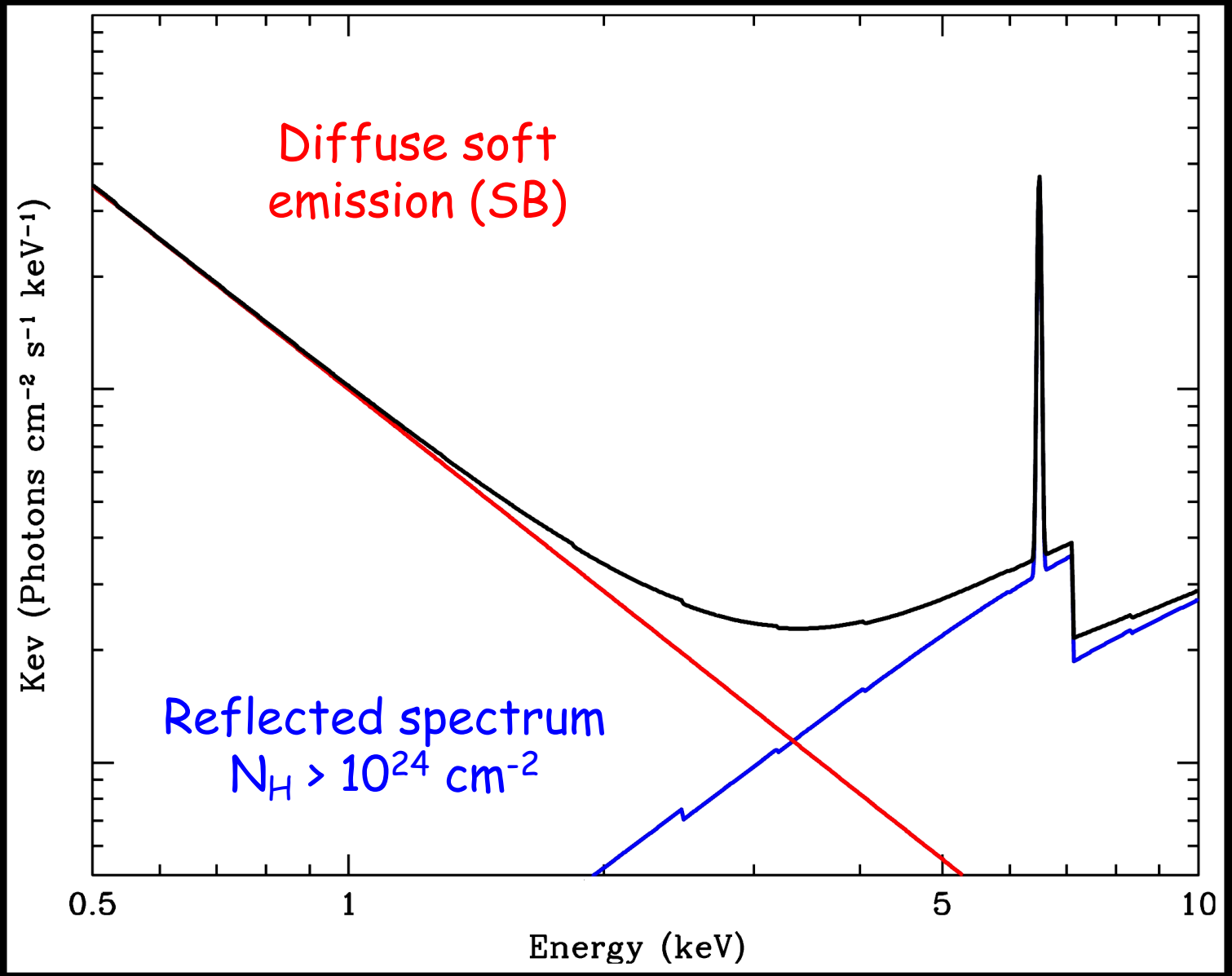

Observed X-ray emission of ULIRGs

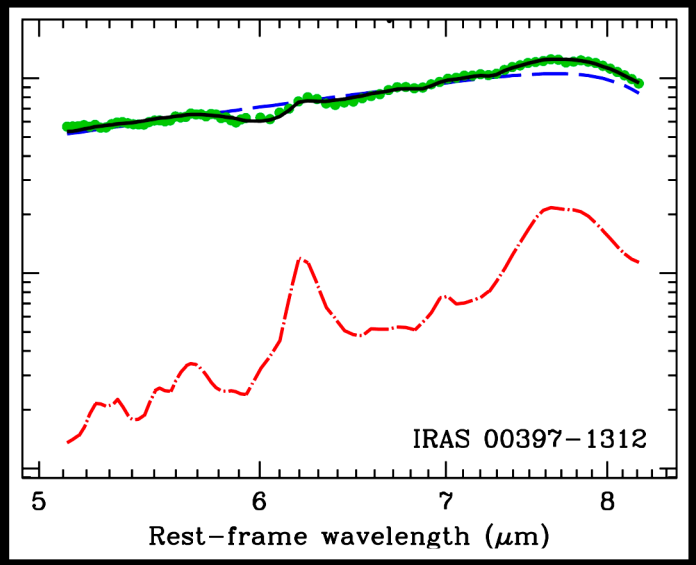

IRAS 00397-1312

$L_{SB} \sim 4 \times 10^{12}\ L_{\odot}$
$L_{AGN} \sim 5 \times 10^{12}\ L_{\odot}$
$(\tau_{6\mu m} \sim 0.25)$

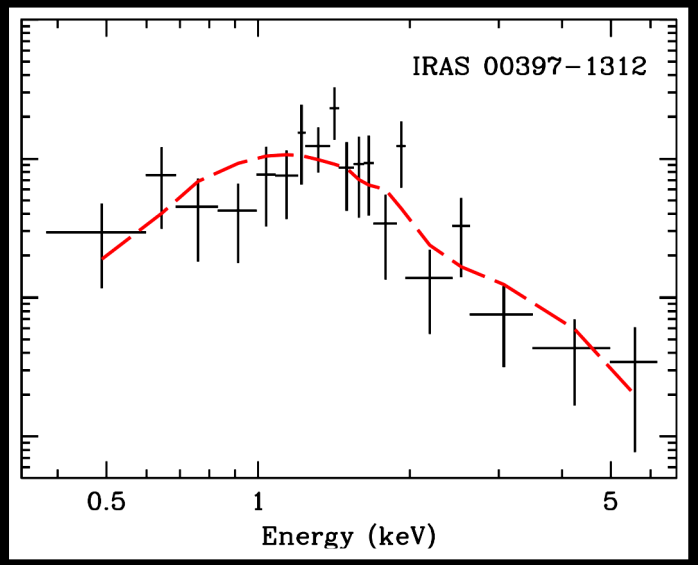

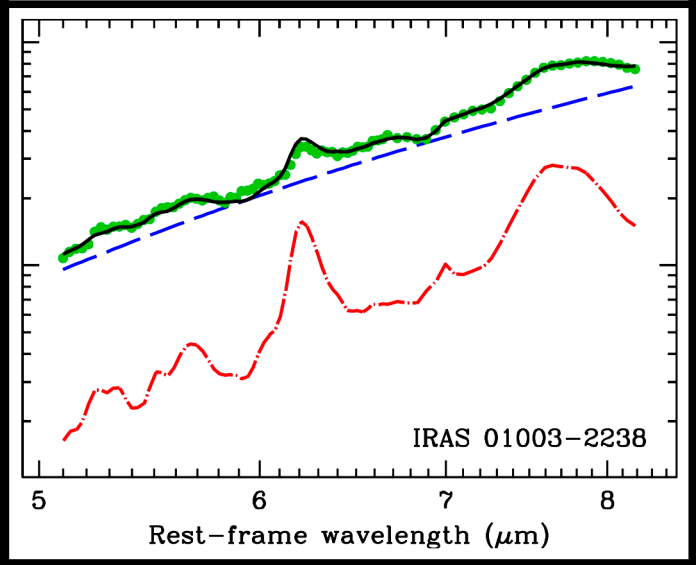

IRAS 01003-2238

$L_{SB} \sim 1 \times 10^{12}\ L_{\odot}$
$L_{AGN} \sim 1 \times 10^{12}\ L_{\odot}$
$(\tau_{6\mu m} \sim 1.6)$

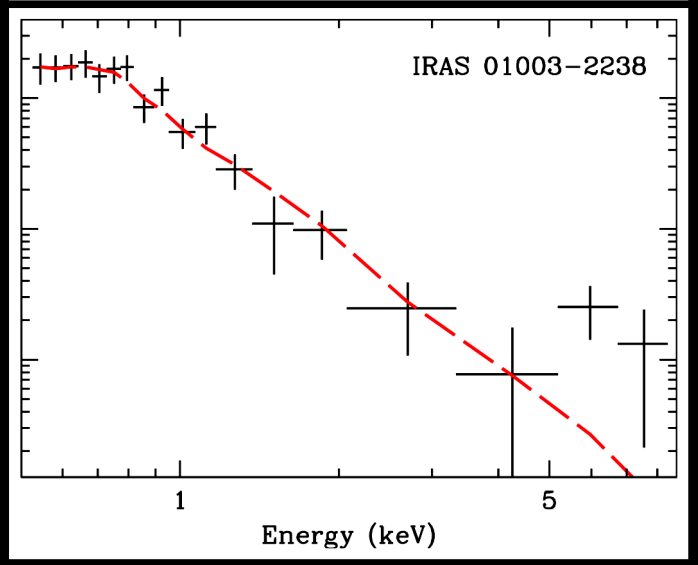

SB as expected but no AGN -> $N_H > 10^{24}$ cm^{-2} and complete covering

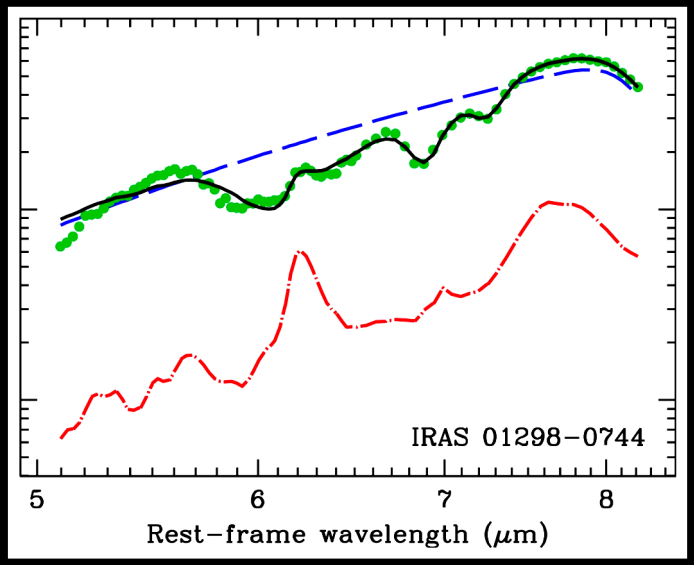

IRAS 01298-0744

$L_{SB} < 6 \times 10^{11}\ L_{\odot}$
$L_{AGN} \sim 2 \times 10^{12}\ L_{\odot}$
$(\tau_{6\mu m} \sim 1.8)$

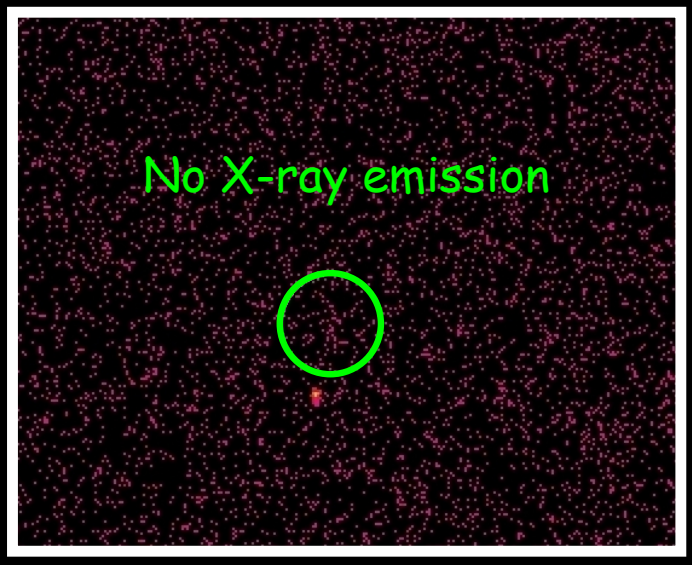

No X-ray detection -> $N_H > 10^{24}$ cm^{-2} and complete covering

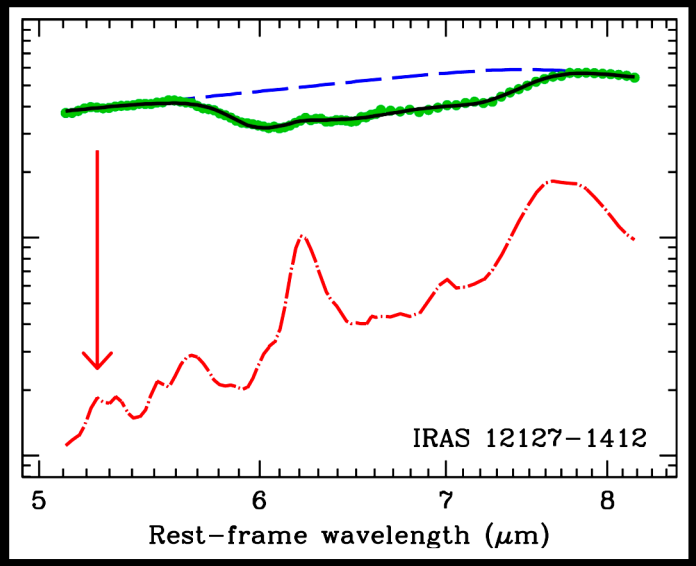

IRAS 12127-1412

$L_{SB} < 2 \times 10^{11}\ L_{\odot}$
$L_{AGN} \sim 1.4 \times 10^{12}\ L_{\odot}$
$(\tau_{6\mu m}\ ?)$

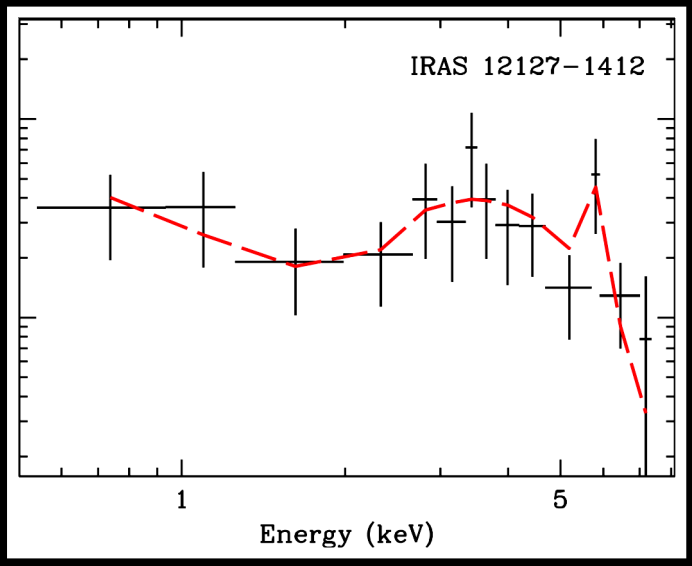

No SB and reflected AGN -> $N_H > 10^{23}$ cm^{-2} and substantial covering

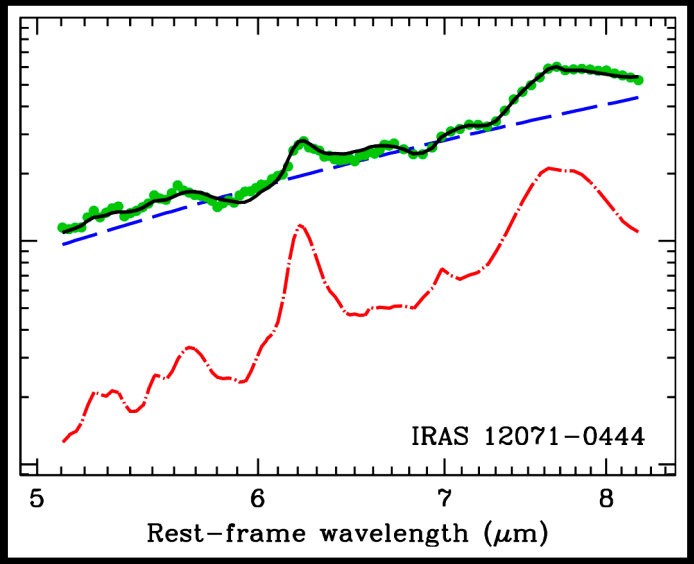

IRAS 12071-0444

L_{SB} ~ 1.5x10^{12} $L_{\odot}$
L_{AGN} ~ 1x10^{12} $L_{\odot}$
($\tau_{6\mu m}$ ~ 1.1)

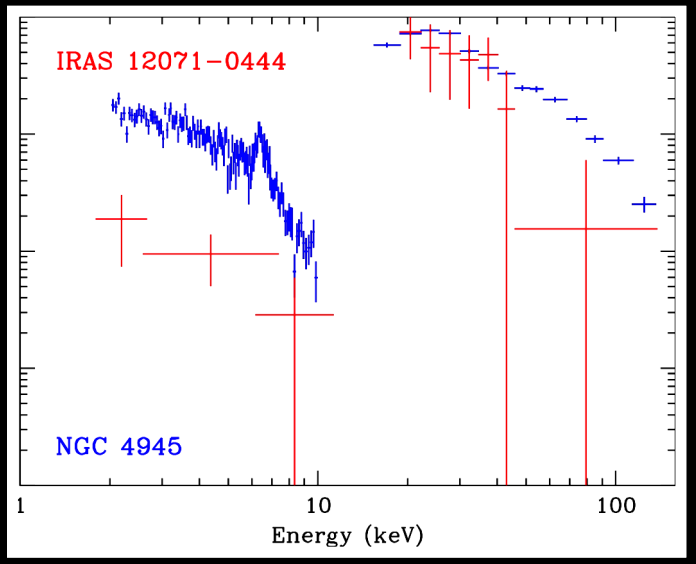

AGN *detected* at E>10keV -> N_H ~ 2x10^{24} cm^{-2} and complete covering

IRAS 00182-7112

L_{SB} < 5x10^{11} $L_{\odot}$
L_{AGN} ~ 9x10^{12} $L_{\odot}$
($\tau_{6\mu m}$?)

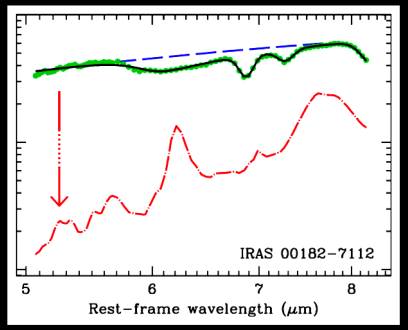

X-rays: Reflected spectrum of a hidden Compton-thick AGN seen through N_H ~ 10^{23} cm^{-2}
(Nandra & Iwasawa 07)

IRAS 08572+3915

L_{SB} ~ 2x10^{11} $L_{\odot}$
L_{AGN} ~ 1.2x10^{12} $L_{\odot}$
($\tau_{6\mu m}$ ~ 0.45)

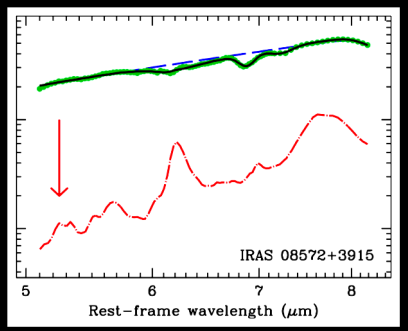

X-rays: *Chandra* 0.5-10keV flux of ~5x10^{-15} erg s^{-1} cm^{-2}, no *Suzaku* detection -> N_H ~ 10^{25} cm^{-2} ?
(Teng+09)

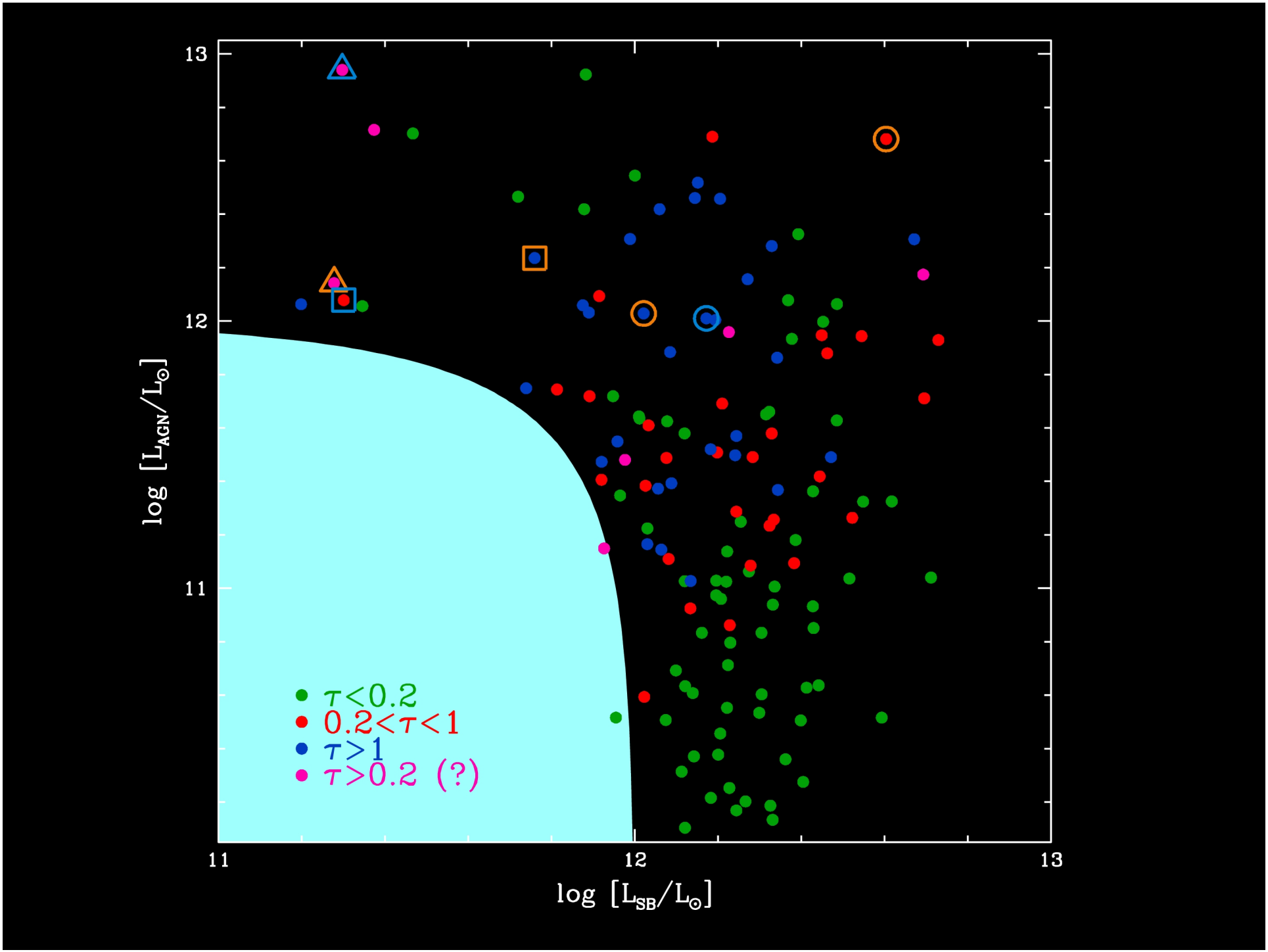
13
12
11
11
12
13
log [L_AGN/L_⊙]
log [L_SB/L_⊙]
τ<0.2
0.2<τ<1
τ>1
τ>0.2 (?)

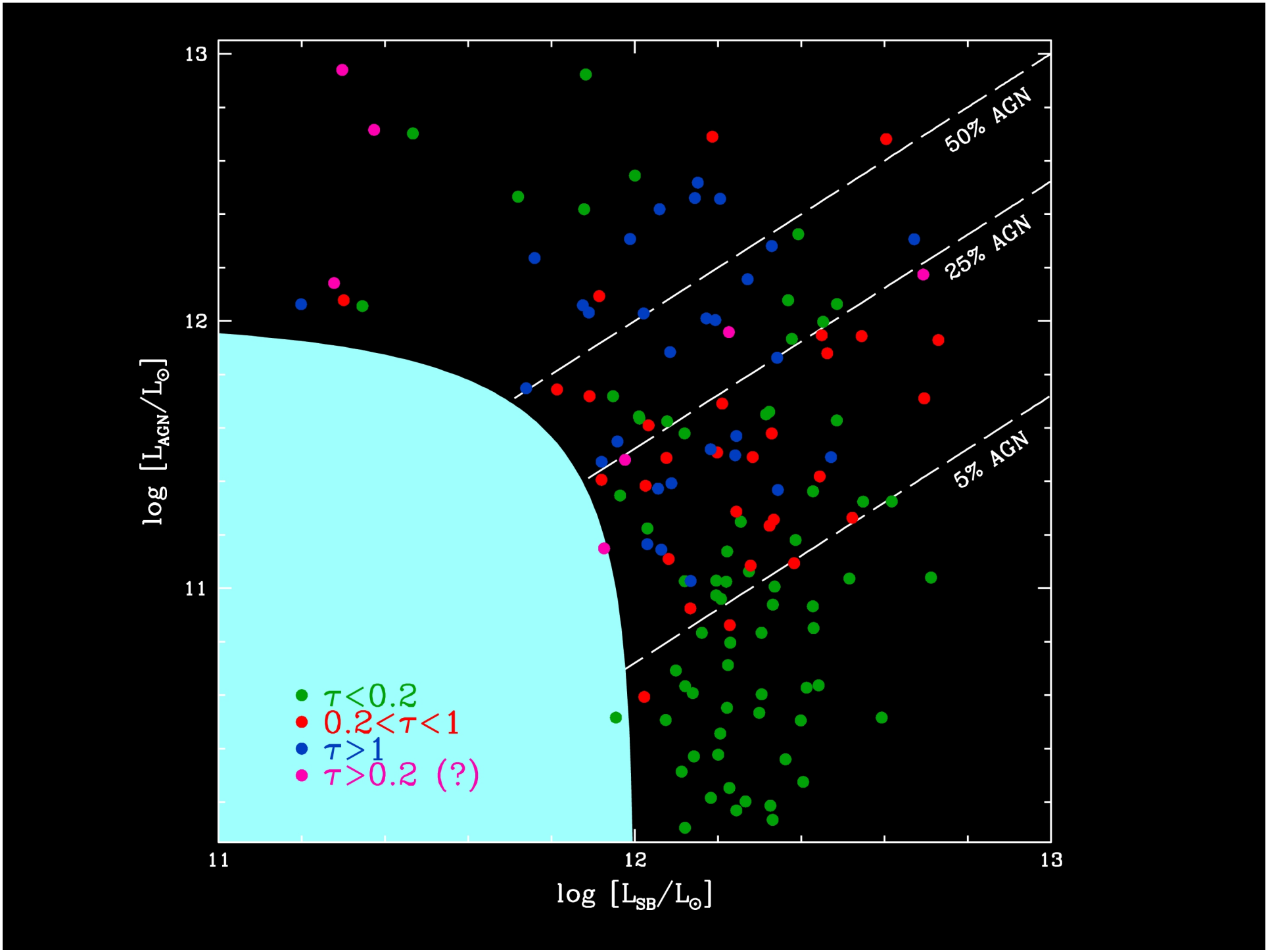
13
12
11
11
12
13
log [L_AGN/L_⊙]
log [L_SB/L_⊙]
50% AGN
25% AGN
5% AGN
τ<0.2
0.2<τ<1
τ>1
τ>0.2 (?)

2. Narrow-Line Seyfert 1 Galaxies

- Definition: FWHM (Hβ) < 2000 km/s
  (Osterbrock & Pogge 85)
- Steep X-ray spectra and soft excess
  (Boller, Brandt & Fink 96)
- Rapid large-amplitude X-ray variability
  (Gallo+04)
- Evidence for large metal abundances
  (Shemmer & Netzer 02)
- Strong FeII emission compared to Hβ
  (Grupe+04)
- Low BH mass and high accretion rate
  (Collin & Kawaguchi 04)

Mid-IR diagnostics: 6.2 *μm* PAH feature against 6 *μm* continuum as tracers of star formation and AGN hot dust component

Comparison between complete samples of NLS1s and BLS1s (59+54 sources, ~6 orders of magnitude in luminosity) to probe SF and BH accretion in type 1 AGN -> different populations?

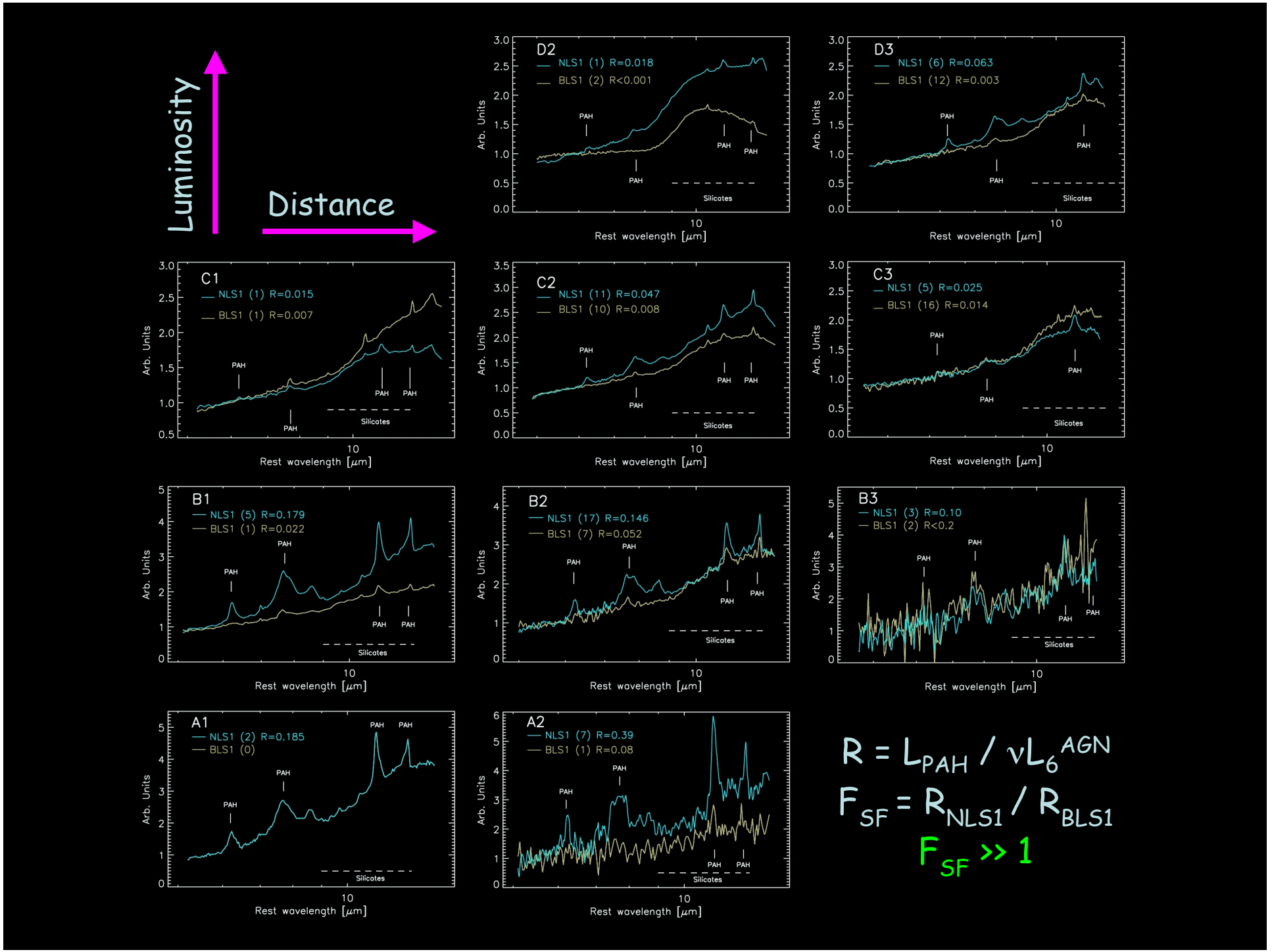
Luminosity
Distance
D2
NLS1 (1) R=0.018
BLS1 (2) R<0.001
D3
NLS1 (6) R=0.063
BLS1 (12) R=0.003
C1
NLS1 (1) R=0.015
BLS1 (1) R=0.007
C2
NLS1 (11) R=0.047
BLS1 (10) R=0.008
C3
NLS1 (5) R=0.025
BLS1 (16) R=0.014
B1
NLS1 (5) R=0.179
BLS1 (1) R=0.022
B2
NLS1 (17) R=0.146
BLS1 (7) R=0.052
B3
NLS1 (3) R=0.10
BLS1 (2) R<0.2
A1
NLS1 (2) R=0.185
BLS1 (0)
A2
NLS1 (7) R=0.39
BLS1 (1) R=0.08
PAH
Silicates
Arb. Units
Rest wavelength [μm]
$R = L_{PAH} / \nu L_6^{AGN}$
$F_{SF} = R_{NLS1} / R_{BLS1}$
$F_{SF} >> 1$

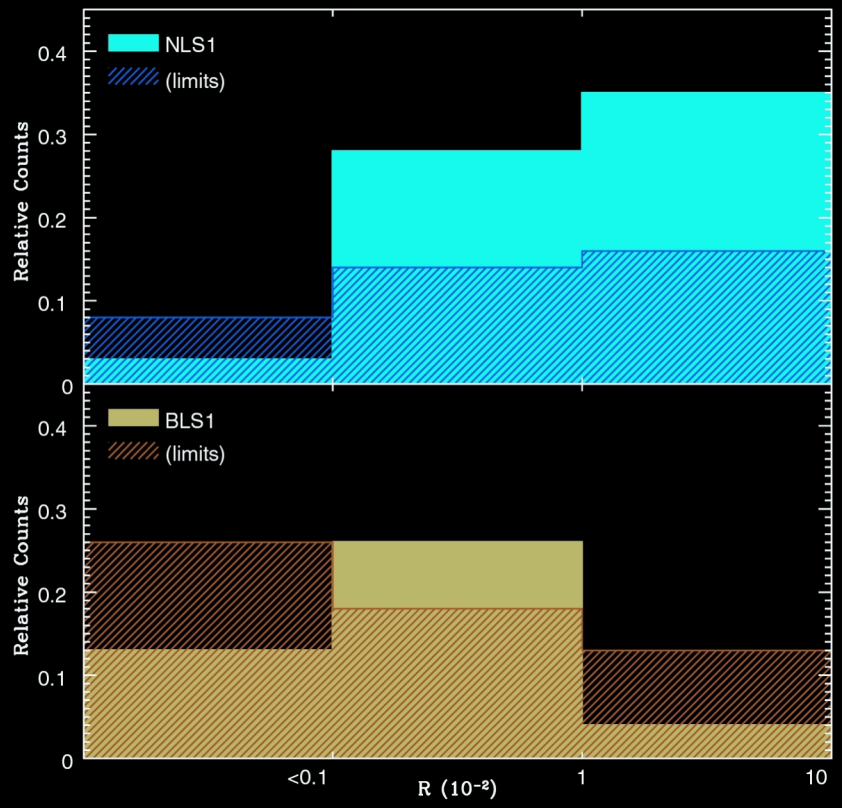

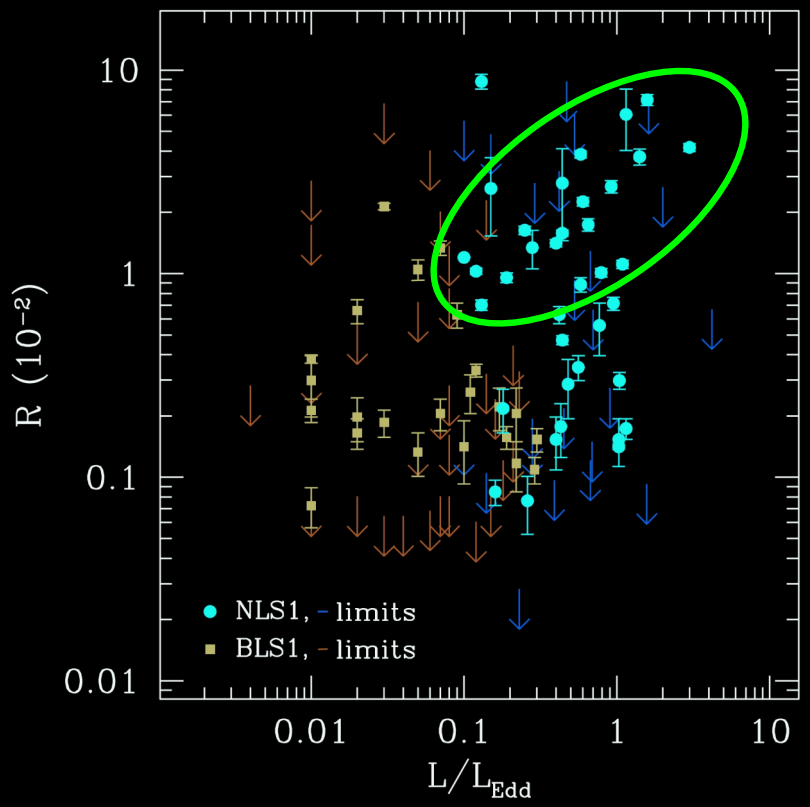

Larger SF activity at low BH masses and high accretion rates: only NLS1s are found at extreme values

Gemini/GMOS IFU observations of NLS1s harbouring the most intense SF to probe metallicity gradients and feedback

Sani, Lutz, Risaliti et al. 2010, MNRAS, 403, 1246

Summary

- Solid constraints to the AGN/SB power balance in local ULIRGs from Spitzer/IRS 5-8 *μm* spectroscopy

- Dominant SB contribution but AGN present in most ULIRGs

- Elusive AGN population not detected at other wavelengths; many of these components are heavily obscured

- Follow-up X-ray observations:
  - agreement with the IR spectral decomposition
  - large fraction of Compton-thick sources
  - evidence for unusually low dust to gas ratios
  - no X-ray reflection: almost complete covering
  - link between AGN obscuration and SB activity?

- PAH detection rate much larger in NLS1s than in BLS1s

- Intense star formation taking place in the circumnuclear environment of high accretion efficiency AGN